Double-Loop Sliding Mode Control of Reentry Hypersonic Vehicle with RCS

JIA Song[1,] CE Hao[1], YANXUE Zhang[1], NANJIA Yu[2], YANG Liu[2], Erfu Yang[3]

***Abstract*— In order to solve the problem of insufficient aerodynamic moment caused by thin air in the re-entry stage of hypersonic vehicle, this paper establishes an attitude angle model of hypersonic vehicle with reaction control system (RCS), and derives its affine linear model to decoupled the internal and external loop. According to the dead zone and saturation characteristics of RCS thruster, a control method to convert continuous moment into discrete switching instruction using pulse width modulation (PWM) is proposed. Since the number of thrusters is usually redundant, the installation matrix of thrusters in the body coordinate is established, and the command moment is coordinately distributed to the individual thrusters. Then a double-loop sliding mode controller (DSMC) is designed to achieve attitude stability and trajectory tracking. Finally, the simulation results show that DSMC has higher maneuverability, fewer thruster switches and stronger robustness to interference.**

I. INTRODUCTION

The reentry hypersonic vehicle(HV) flies across the atmospheric space of 25km~100km above sea level and at a hypersonic speed more than Mach 5 with high maneuverability and large flight envelope, which plays an irreplaceable role in both martial attraction and low cost transportation between space and the earth [1,2]. However, due to the low density of the upper atmosphere and insufficient aerodynamic moment, the jet thruster is necessary to provide extra moment. Therefore, Reaction Control System (RCS) of reentry aircraft should be taken into consideration [3].

In recent years, researchers mainly design the HV longitudinal model's control system. Literatures [4,5] use backstepping sliding mode control to finish the maneuvering task by using the pneumatic rudder surface, but the thin atmosphere has not been considered. In literature[6,7], both of them mention terminal sliding mode control (TSMC) method, while the former detailed calculated longitudinal model of TSMC surface coefficient and control, which realize the fast track of longitudinal velocity and height, the later one fully demonstrated the HV 6-DOF model, taking attitude angle as the controlled target and finally the error is reduced to 0.03°.

At the same time, many scholars considered the shortage of aerodynamic force, they use rudder surface and thruster together, designing hybrid RCS and to reasonably distribute moment. Through engineering experience, the distribution law is sufficiently demonstrated in literature [8] by using fuzzy logic control method. In literature[9], a segmented function is designed to distribute moment, and the RCS gradually exits with the reentry process, so that the pneumatic rudder works.

*This work is supported by Key Laboratory of Spacecraft Design Optimization and Dynamic Simulation Technologies, Minisitry of Education, China.

1.JIA Song and CE Hao, are with School of Astronautics, Beihang University, Beijing, China (email: haoce@buaa.edu.cn).

3. Erfu Yang is at the Space Mechatronic Systems Technology Laboratory, Department of Design, Manufacture and Engineering Management, University of Strathclyde, Glasgow, UK.

In addition, [11,12] mentioned that the installation position and angle of thrusters have different influences on the moment generated by the center of mass, and the components of each thruster are obtained to the HV through the decomposition of thrust. In [9] it also discusses the hysteresis characteristics of the discrete switch of the thruster, therefore PWPF is adopted to optimize and reduce the switching times.

The purpose of this paper is to maintain the attitude stability of HV reentry segment with RCS. Based on the former mentioned assumptions, the following assumptions are made [10]:

(1) The RCS thruster is installed in a fixed position and provides a constant thrust, with only two switching states.

(2) Through the model simulation state ,50 km above the upper atmosphere, air density is lower than 0.01 kg/m3 which leads to the aerodynamic moment is far less than the thruster (less than 0.1%).

(3) The HV attitude angle change rate is seriously coupled, and the triaxial rotation must be considered comprehensively for attitude stability.

According to assumptions above, analysis of HV RCS dynamic system and controlling strategy for thrusters are necessary for reentry segment stability. The remainder of the paper is organized as follows. In section 2, attitude angle model with RCS for HV is established. In section 3, installation matrix and reform PWM for RCS are proposed to convert expected moment to discrete moment on each thruster. In section 4, the double-loop SMC algorithm is introduced to stable the altitude angle. In section 5, verification simulation analysis results are shown. Finally, Section 5 draws conclusions.

II. HYPERSONIC VEHICLE MODEL WITH RCS

A. Nonlinear Model for HV

The Winged-Cone model of HV is obtained as the basic aerodynamic layout. Its airfoil contains triangular wing, vertical tail wing, folding horizontal canard wing and longitudinal lateral thrust vector [12], as figure 1.

On the basis of aerodynamic force, the aircraft model is changed into RCS model, and only attitude Angle and angular velocity are considered for description. The form is shown in equation (1):

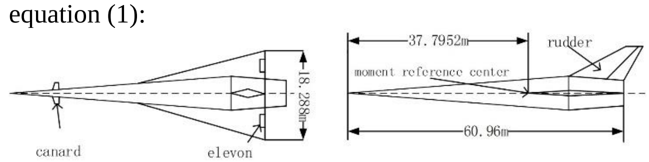

Figure 1. Top and side views of the Winged-Cone aircraft

$$\dot{\alpha} = \frac{1}{Mv\cos\beta}(-L + Mg\cos\gamma\cos\mu - T_{rx}\sin\alpha + T_{rz}\cos\alpha) + q - \tan\beta(p\cos\alpha + r\sin\alpha)$$

$$\dot{\beta} = p\sin\alpha - r\cos\alpha + \frac{1}{Mv}(Y\cos\beta + Mg\cos\gamma\sin\mu - T_{rx}\sin\beta\cos\alpha + T_{ry}\cos\beta - T_{ry}\sin\beta\sin\alpha$$

$$\dot{\mu} = \sec\beta(p\cos\alpha + r\sin\alpha) + \frac{1}{Mv}[L\tan\gamma\sin\mu - Mg\cos\gamma\cos\mu\tan\beta + L\tan\beta + (T_{rx}\cos\alpha - T_{rz}\cos\alpha)\ (\tan\gamma\sin\mu + \tan\beta) - (T_{rx}\cos\alpha + T_{rz}\sin\alpha)\tan\gamma\cos\mu\sin\beta + (Y + T_{ry})\tan\gamma\cos\mu\cos\beta] \quad (1)$$

$$\dot{p} = -\frac{I_{zz} - I_{yy}}{I_{xx}}qr + \frac{1}{I_{xx}}(l_A + l_{Tr})$$

$$\dot{q} = -\frac{I_{xx} - I_{zz}}{I_{yy}}pr + \frac{1}{I_{yy}}(m_A + m_{Tr})$$

$$\dot{r} = -\frac{I_{yy} - I_{xx}}{I_{zz}}pq + \frac{1}{I_{zz}}(n_A + n_{Tr})$$

Six state variables for the dynamic equation are $x = [\alpha, \beta, \mu, p, q, r]^T$, respectively as the angle of attack, sideslip angle, roll angle, roll angle rate, pitching angle rate and yaw angular rate. I_{xx} represents the moment of inertia in the X-axis direction in body coordinate system.

Different from the general model, the control force of this model is divided into two parts,: aerodynamic moment and RCS moment in which L, Y, Drepresent lift force, lateral force and resistance, while T_{rx}, T_{ry}, T_{rz} represent the integrated discrete force in the X, Y and Z directions of the body system. Correspondingly, l_A, m_A, n_A and l_{Tr}, m_{Tr}, n_{Tr} represents the aerodynamic and RCS torques on the three axes of the system respectively. The aerodynamic moment calculation is as follows[3]:

$$D = qSC_D$$
$$Y = qSC_Y$$
$$L = qSC_L$$
$$l_A = qbSC_l$$
$$m_A = m_{mrc} - X_{cg}Z \quad (2)$$
$$n_A = n_{mrc} - X_{cg}Z$$
$$q = \frac{1}{2}\rho v^2$$

Where, Z represents the distance between barycenter and press center while m_{rcs} and n_{rcs} are moment from thrusts in Y and Z direction.

B. *Affine Model for HV*

It can be clearly judged from the HV RCS model that the system has strong coupling and is a complex nonlinear system, which undoubtedly causes many difficulties in analyzing its stability and designing control methods. Therefore, in this paper, affine linear model is obtained by affine transformation, and the attitude angle and triaxial angular rate are taken as state variables to separate the fast and slow control loops. The affine linear form is as follows:

$$\dot{\Omega} = f_s + g_s\omega + g_{s1}\delta + g_{s2}T_r$$
$$\dot{\omega} = f_f + g_f M_c \quad (3)$$

Where, $\Omega = [\alpha, \beta, \mu]^T$, $\omega = [p, q, r]^T$ and $\delta = [\delta_e, \delta_a, \delta_r]^T$are the pneumatic rudder surface deflection angle, $T_r = [T_{rx}, T_{ry}, T_{rz}]^T$ represents the vector of control force provided by RCS. In the model, $M_c = [l_{aero}, m_{aero}, n_{aero}]^T$ are the roll, pitch and yaw moment , including $M_{RCS} = [l_{ctrl}, m_{ctrl}, n_{ctrl}]^T$ as RCS moment vector control, which shown as equation (4):

$$M_c = g_{f,\delta}\delta + M_{RCS} \quad (4)$$

Specific expressions of each coefficient g can be referred to[13]. The main target of reentry control system is to assure a suitable rudder angle δ and RCS control strategy, to improve the speediness and accuracy of the attitude angle Ω track its expected value Ω_c.

The pneumatic actuator and control of RCS for $\dot{\alpha}, \dot{\beta}, \dot{\mu}$ are relatively smaller, which can be ignored in the affine model. Eventually, the equation (3) can be simplified as equation (5):

$$\dot{\Omega} = f_s + g_s\omega$$
$$\dot{\omega} = f_f + g_f M_c \quad (5)$$

The two formulas have an obvious speed difference on the time scale. With the theory of singular value perturbation, HV reentry attitude control are divided into fast loop and slow loop, serving attitude angle $\Omega = [\alpha, \beta, \mu]^T$ as the slow system state variables, and $\omega = [p, q, r]^T$ as fast system state variables. Consequently, it is necessary to design separate control instructions for two separate loops.

The target of slow loop is to obtain command angular rate ω_c based on expected attitude angle Ω_c, and using Ω_c to design suitable control moment M_c in the fast loop. Finally, moment is distributed to rudder deflection angle δ_c and RCS thrust $M_{rcs}$to generate attitude control for the HV. The double-loop structure is shown in the figure 2 below:

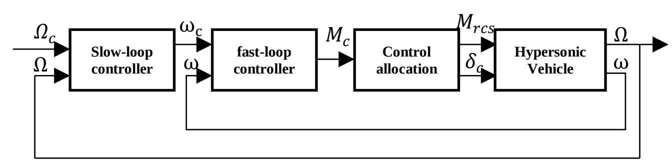

Figure 2. HV controller double-loop structure

III. RCS Thrusters Design

The RCS thruster is solidly connected to the aircraft body, and there are only two states of switch. Therefore, thrusters need to be installed in multiple directions in the HV to provide triaxial moment. Meanwhile, the thrusters cannot provide continuous moment, so the control law design is necessary to make the continuous moment equivalent to discrete form.

A. *Analysis of thruster installation mode*

Due to the different installation Angle and position of propeller, different thrust and moment will be generated. Multiple thruster combined provide triaxial moment.

As shown in the figure 3, along the yoz plane of the body axis, the thrust F and the Y-axis angle is α, and the vertical distance from the center of mass is d. In the xoz plane, the distance between thrust F and the center of mass O is L.

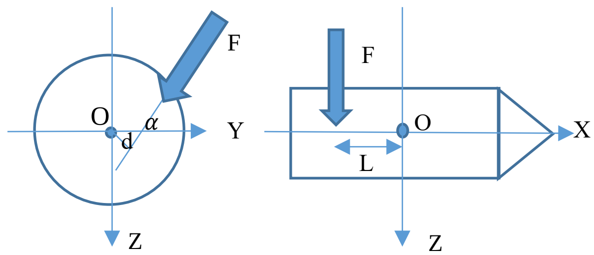

Figure 3. Thruster installation model

According to the trig function, the thrust and moment of the three axes can be obtained as follows equation (6):

$$
\begin{aligned}
F_x &= 0\\
F_y &= -Fcos\alpha\\
F_z &= Fsin\alpha\\
M_x &= Fd\\
M_y &= FLsin\alpha\\
M_z &= FLcos\alpha
\end{aligned}
\tag{6}
$$

As can be seen from the above equation, when α is not zero, control force will be generated on Y and Z axis, which not only changes the flying attitude, but also makes the HV subject to deflection force. Therefore, when controlling the X-axis moment, a set of thrusters symmetric about the origin can be used to eliminate the impact of additional Y-axis and Z-axis thrust. However, when Y and Z-axis moment control is carried out, thrust to the center of mass must be introduced, which needs to rely on the self-stability of the HV or compensation by symmetrical thruster. This part can be solved by control algorithm.

Suppose the total number of thrusters of HV is N, where i represents the label of the thruster. The Y-axis angle of each thruster is α_i, the center distance d_i, the distance from the center of mass L_i, and the thrust F_i. $T_{rcs}i$ is the thrust installation matrix for each thruster, shown as equation(7):

$$
\begin{aligned}
T_{rcs}i = [0 \quad -F_i cos\alpha_i \quad F_i sin\alpha_i \\
F_i d_i \quad F_i L_i sin\alpha_i \quad F_i L_i cos\alpha_i]^T
\end{aligned}
\tag{7}
$$

T_{rcs} is the installation matrix of the entire HV:

$$T_{rcs} = [T_{rcs}1 \quad T_{rcs}2 \quad \ldots \quad T_{rcs}N]^T \tag{8}$$

At the same time, the state of the switch thruster only has two states-on and off,, set the state matrix u_{rcs} component $u_{rcs}i$ of each thruster can only be 0 or 1, where:

$$u_{rcs} = [u_{rcs}1 \quad u_{rcs}2 \quad \ldots \quad u_{rcs}3]^T \tag{9}$$

Then, the triaxial thrust and triaxial moment generated by the jet thruster are set as:

$$FM_{rcs} = [F_x \quad F_y \quad F_z \quad M_x \quad M_y \quad M_z]^T \tag{10}$$

The three matrixes are related as follows:

$$FM_{rcs} = T_{rcs} u_{rcs} \tag{11}$$

Thus, given the current thruster switch state, corresponding thrust and moment can be obtained. In fact, in the process of designing the control system, the expected moment will be obtained firstly and the actual switch control will be solved in reverse. However, a highly reliable RCS system thruster design is redundant for the number of thrusters more than degree of freedom, namely N>6. The installation matrix T_{rcs} is irreversible, and the least squares solution can be acquired by solving the pseudo inverse, as equation (12) shows:

$$u_{rcs} = (T_{rcs})^T [T_{rcs} (T_{rcs})^T]^{-1} FM_{rcs} \tag{12}$$

Finally, the expected moment of control is transformed into a continuous thrust instruction for each thruster through the installation matrix, and afterwards the continuous instruction is decentralized by the method of pulse width modulation.

B. Reformed thruster moment PWM

The RCS use thrusters for attitude control, which solves the problem of insufficient aerodynamic force in the early stage of reentry. Since thrusters can only provide constant thrust and cannot provide variable torque, in order to meet the output of command moment, switch instruction needs to be divided into discrete cases. Continuous moment is converted into discrete moment through pulse width modulation (PWM) [14,15].

The basic principle of PWM control is that narrow pulses (rectangles or trapezoids) with equal impulse but different shapes have the same control effect when they are added to the system with inertial link. The continuous moment is M(t), and discrete moment is $\bar{M}$. The width of the pulse for the n sampling period is τ_n, thus the principle can be explained as following equation (13):

$$\int_{(n-1)T}^{nT} M(t)dt = \bar{M}\tau_n \tag{13}$$

However, the solenoid valve, through the relay power on and off leading to solenoid valve suction and release, mainly controls thruster switch. Therefore, there is a delay between opening and closing instruction.

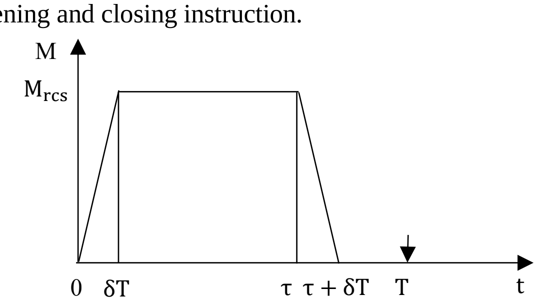

Figure 4. The thruster switching characteristic curve

As shown in the figure 4, each instruction period is T. In the current period t=0s time to open the thruster, because the relay is energized to attract the solenoid valve needs a certain time δT, the thrust F in a very short period of time from 0 to the peak M_{rcs}. Afterwards, the thruster is in the on state until the instruction opens at the time of instruction $\tau + \delta T$, and the instruction to close the thruster is issued. After the same shutdown time, the thruster will return to 0 and end the instruction cycle with the shutdown state.

According to the thruster response curve in figure. 4, it can be obtained from the impulse equivalence that the area surrounded by the moment profile and the time axis is the impulse, So we use formula (13) to derive formula (14):

$$\frac{M_{rcs}[(\tau+\delta T)+(\tau-\delta T)]}{2}=M_c\cdot T$$
$$\tau=\frac{M_c}{M_{rcs}}T \tag{14}$$

The repeated opening and closing of thruster in each instruction cycle is easy to cause fuel waste and mechanical failure, so two special cases are considered to reduce the number of repeated opening and closing.

As for the dead zone, when the aircraft is in the vicinity of the command attitude angle balance, the command moment obtained by the control rate may be very small, and the propeller instruction finally obtained by pulse width modulation will be opened only for a short time $\tau < \delta T$ as in figure 5:

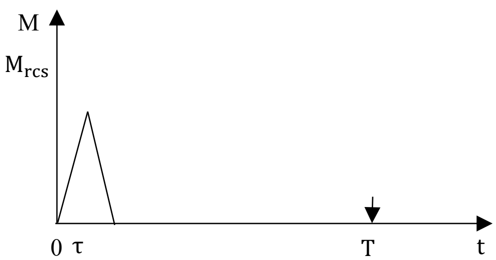

Figure 5. The dead zone condition

In this case, the thruster moment has not reached the maximum, and the modulating moment has not reached the command moment requirements. Therefore, instructions need to be set to open the time dead zone. Improved instruction opening time as shown in the equation (15):

$$\tau_0=\frac{M_c}{M_{rcs}}T \quad \tau=\begin{cases}\tau_0 & ,\delta T<\tau_0<T\\ 0 & ,\tau_0<\delta T\end{cases} \tag{15}$$

Secondly, we consider the condition of thrust saturation. In the reentry HV design process, it is necessary to consider whether the RCS thruster can provide sufficient control moment. If a single thruster fails to meet the moment requirements, multiple thrusters will be turned on and the thruster will be kept continuously open, which is the continuous opening state generated by the saturation of the thruster.

When the instruction opens the time $\tau_0 > T-\delta T$, it can be used to prevent the thruster from being closed in the current period and there is no instruction to open the thruster in the next period. However, the instructed opening time τ should also be calculated for the next period to determine whether the signal to close the thruster should be given within this period.

Considering the dead zone and saturation problems comprehensively, the instruction opening time is divided into three nonlinear functions according to the instruction moment, and its expression is shown in formula (16):

$$\tau_0=\frac{M_c}{M_{rcs}}T \quad \tau=\begin{cases}\tau_0 & ,\delta T<\tau_0<T\\ 0 & ,\tau_0<\delta T\\ T & ,\tau_0>T-\delta T\end{cases} \tag{16}$$

After installation matrix solution and improving PWM method of thruster, the command moment M_c is decomposed into the opening time τ_i of each thruster in each period, which can be directly used for the computer to send control instructions.

IV. Double-loop SMC for HV

Sliding mode control (SMC) is a variable structure control algorithm proposed in 1950s. Sliding mode control is a kind of variable structure control method of nonlinear model. The difference between this control method and other control strategies is that the system structure is not fixed, but the dynamic process intentionally forces the system to follow the "sliding mode" trajectory set previously when the current state of the system changes[16].

A. *Asymptotically convergent SMC*

The most traditional sliding mode control is the first order sliding mode[17]. Considering the following nonlinear system, a first-order sliding mode controller is designed to make the system approach the equilibrium surface:

$$\dot{x}=f(x)+b(x)u,\ u\in R \tag{17}$$

In this system, $s(x)\in R$ of the sliding mode surface is the most commonly used linear function, and $s(x)=cx$. In this case, the derivative of $s(x)$ on the track surface of the system is taken. If partial $\frac{\partial s(x)}{\partial x}b(x)$ is non-singular, the SMC law based on the approach law can be adopted. The surface and derivation shown as equation (18):

$$\dot{s}(x)=c\dot{x}$$
$$\dot{s}(x)=c\left[\frac{\partial s(x)}{\partial x}f(x)+\frac{\partial s(x)}{\partial x}b(x)u\right] \tag{18}$$

Constant velocity approach law $\dot{s}(x)=-\eta sig(s(x))$, $\eta>0$ is adopted, we transform equation (17) into (18) to get control strategy u as:

$$c\left[\frac{\partial s(x)}{\partial x}f(x)+\frac{\partial s(x)}{\partial x}b(x)u\right]=-\eta sig\big(s(x)\big)$$
$$u=-\left(\frac{\partial s(x)}{\partial x}b(x)\right)^{-1}\left[\frac{\partial s(x)}{\partial x}f(x)+\frac{\eta}{c}sig(s(x))\right] \tag{19}$$

It is proved that the sliding mode surface can be reached and the system is asymptotically stable by means of lyapunov function.

Select lyapunov function $V=\frac{1}{2}s^2$, the derivation is $\dot{V}=s\dot{s}=-\eta|s|$, thus the motion of the system is always close to the sliding mode surface, and can reach the sliding surface in finite time. The system dynamics after reaching the sliding mode surface will be uniquely determined by the equation $s(x)=0$. When using the linear sliding mode surface $s(x)=cx$, the system state is asymptotically stable with respect to the equilibrium point.

B. *First order SMC for affine model*

According to the HV affine model mentioned above, the first order sliding mode control based on the constant velocity approach law is made for the fast and slow loops respectively, and the control law is designed.

The system equation as (20):

$$\dot{\Omega} = f_s + g_s\omega + \varphi_s$$
$$\dot{\omega} = f_f + g_f M_c + \varphi_f \quad (20)$$

φ_s and φ_f respectively perturbation interference in the slow and fast loop, caused by uncertainty. Their upper bounds are M_s and M_f

C. Slow loop design

Select the integral sliding surface:

$$\sigma_s = e_s + c_s \int_0^t e_s \, d\tau \quad (21)$$

In the formula, $e_s = \Omega - \Omega_c$ is the error of attitude angle, Ω_c is control angle signal in the slow loop, c_s is a weight to adjust. We take the derivative of the sliding surface, and we get equation (22):

$$\dot{\sigma_s} = \dot{e_s} + c_s e_s$$
$$\dot{\sigma_s} = \left(f_s + c_s e_s - \dot{\Omega}_c\right) + g_s\omega + \varphi_s \quad (22)$$
$$\dot{\sigma_s} = F_s + g_s\omega + \varphi_s$$

Where, $F_s = f_s + c_s e_s - \dot{\Omega}_c$.

According to the control law of first-order sliding mode control, the command angular acceleration is taken as the control quantity of the system's fast channel, and the solution is equation (23):

$$\omega_c = g_s^{-1}\left(\dot{\Omega}_c - f_s - c_s e_s - \eta_s sig(\sigma_s)\right) \quad (23)$$

In the equation, $\eta_s > M_s$. It can resist the influence of model perturbation interference and ensure the slow loop to track the sliding surface movement.

D. Fast loop design

The design process of the fast loop is similar as above. Firstly, we select the integral sliding surface:

$$\sigma_f = e_f + c_f \int_0^t e_f \, d\tau \quad (24)$$

Where $e_f = \omega - \omega_c$ is the error of attitude angle rate, ω_c is control angle rate signal in the fast loop, c_f is a weight to adjust. We take the derivative of the sliding surface, and we get equation (25):

$$\dot{\sigma_f} = \dot{e_f} + c_f e_f$$
$$\dot{\sigma_f} = \left(f_f + c_f e_f - \dot{\omega}_c\right) + g_f M_c + \varphi_f \quad (25)$$
$$\dot{\sigma_f} = F_f + g_f M_c + \varphi_f$$

Where, $F_f = f_f + c_f e_f - \dot{\omega}_c$.

Take the command moment as the control of the system's slow loop, and get equation (26):

$$M_c = g_f^{-1}\left(\dot{\omega}_c - f_f - c_f e_f - \eta_f sig(\sigma_f)\right) \quad (26)$$

Finally, the double-loop SMC control angular velocity and control torque based on HV affine model are given by formulas (23) and (26). Specifically, the $\dot{\omega}_c$ in (26) is derived from (23) ω_c with direct derivation.

V. Simulation and Analysis

The reentry stage of hypersonic aircraft requires a maneuver on the attitude to maintain a high angle of attack attitude to restrict the speed, and to keep lateral attitude stability. According to this requirement, RCS control system of reentry HV is simulated and analyzed.

The initial condition of the simulation is:

$x = y = 1000m$, $H = 60km$, $v = 4800m/s$,

$\chi = \gamma = 0$, $\alpha = 6°$, $\beta = 1°$, $\mu = 3°$, $p = q = r = 0$,

$T_{rx} = T_{ry} = T_{rz} = 0$, $l_{T_r} = m_{T_r} = n_{T_r} = 0$,

$\delta_e = \delta_a = \delta_r = 0°$

The reentry HV needs a high angle of attack to reduce the flight speed, so the control command is:

$\alpha = 45°$, $\beta = 0°$, $\mu = 0°$

In this paper, Simulink is used for simulation. Firstly, it is assumed that HV is not subject to external interference and only the thruster is used for attitude control. The simulation results of its three axes are shown in figure 6. And the control process is divided into two stages: approach sliding mode surface and surface tracking.

.

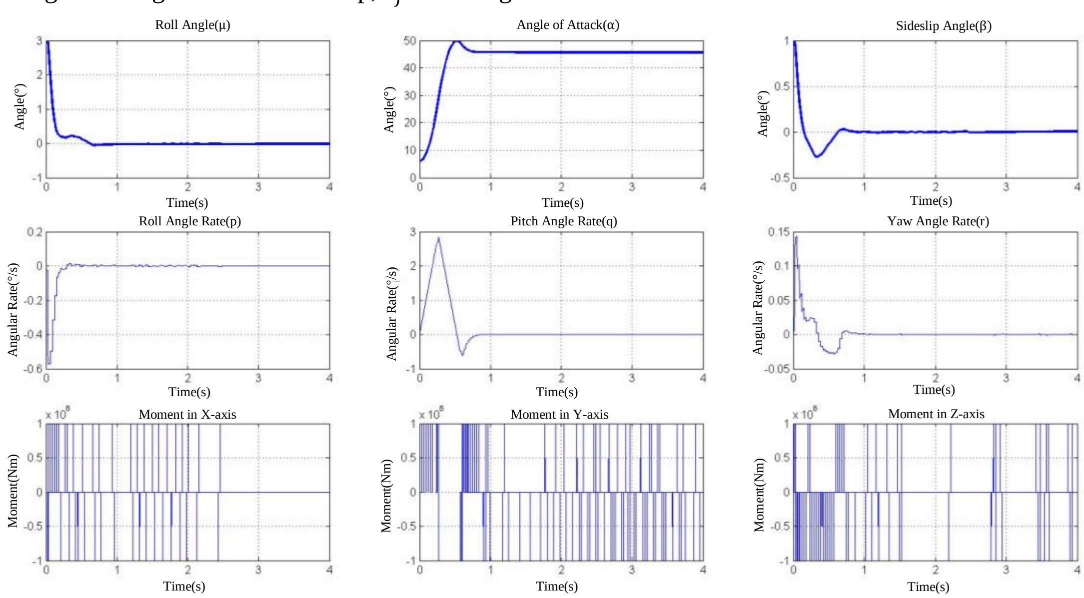

Figure 6. Double-loop SMC reentry HV simulation

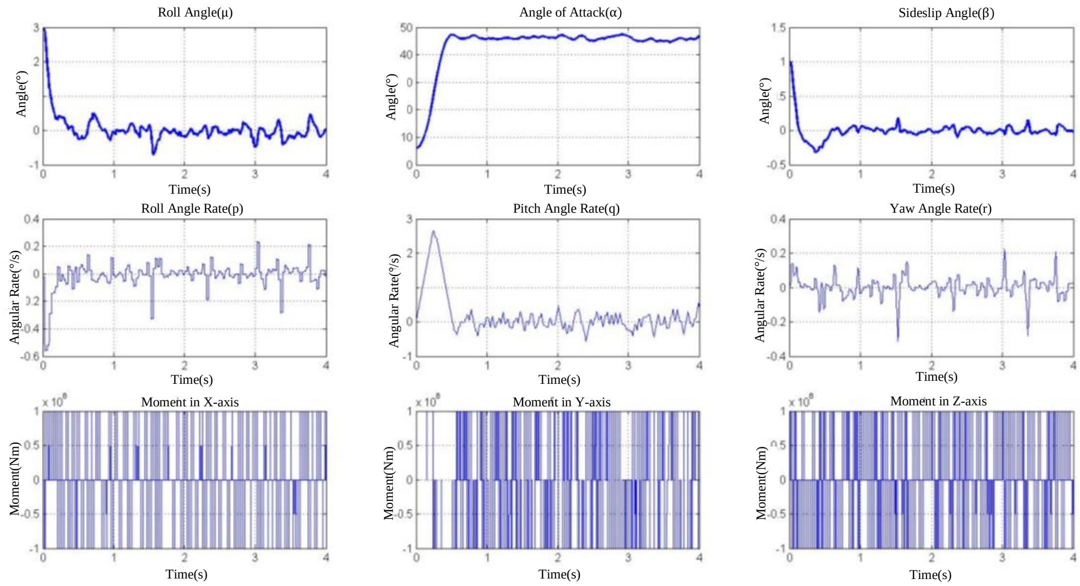

Figure 7. Double-loop SMC reentry HV simulation under interference

In the approaching period, the three attitude angles reach the expectation within 0.7s. The angle of attack and sideslip angle appear overshoot and immediately rebound to equilibrium. And in this time, the thruster performs frequent switching operations to complete the task of rapid maneuver.

In the sliding period, the attitude angles keep still and the thrusters open occasionally to adjust tiny errors. Due to the reformed PWM, the short period of opening control is neglected, which reduce the meaningless short-time opening.

In order to compare and analyze the anti-interference ability of double-loop SMC, the interference moment that obeys gaussian distribution is set in all three axes, and the simulation is carried out in this case. The results are shown in figure 7.

In the disturbed state, the insensitivity of the sliding period near the equilibrium state to disturbance and rapid recovery are very important.

While HV meets interference, the attitude changes, and the system state is far away from the sliding mode surface. The control command is generated to quickly stabilize the state. Therefore, the thruster will be turned on repeatedly to resist interference. According to the analysis in the figure7, the attitude angle can always keep convergence and does not enlarge with the coupling of the three axes, so it has good stability

CONLUSIONS

This paper studies the reaction control system (RCS) of hypersonic vehicle (HV) reentry segment. Based on the Wing-cone model, we establish the attitude angle motion and dynamics equation, and constructs its affine linear form, giving the control system designing scheme of decoupling control of fast and slow loop.

According to the characteristics of RCS thruster, the thruster installation matrix in this system is obtained, and the scommand moment is distributed to each thruster with quantitative redundancy in the form of pseudo-inverse solution. An improved PWM algorithm is adopted to calculate the continuous command moment as the opening time of the thruster. After optimization, invalid opening and closing operations are reduced.

Then, Double-loop SMC algorithm is designed, and control instructions for fast and slow loops are calculated respectively, using integral sliding mode surface based on the affine model. Under the condition of no interference and interference, the simulation of the reentry RCS shows that it can approach quickly in the approaching period and has the ability of interference resistance in the sliding period. Therefore, double-loop SMC algorithm designed in this paper can complete the HV reentry attitude maneuver and attitude stability tasks excellently.

REFERENCES

[1] Jiaxin, Liu , H. Yingdong , and X. Zhihua . “Simulation analysis of hypersonic vehicle flight control based on back-stepping and dynamic inversion.” *Control Conference IEEE*, 2014.

[2] Fidan, Barıs, M. Mirmirani , and P. A. Ioannou . “Flight Dynamics And Control Of Air-Breathing Hypersonic Vehicles: Review And New Directions.” *AIAA International Space Planes & Hypersonic Systems & Technologies* 2015.

[3] Li huifeng. “Hypersonic vehicle guidance and control technology”. *China Aerospace Publishing Press*, 2012.

[4] An, Hao , et al. “Approximate Back-Stepping Fault-Tolerant Control of the Flexible Air-Breathing Hypersonic Vehicles.” *IEEE/ASME Transactions on Mechatronics* (2015):1-1.

[5] Wang, F. , et al. “Approximate backstepping sliding mode control for a flexible air-breathing hypersonic vehicle.” *Control Conference IEEE*, 2013.

[6] Hu, Xiaoxiang , et al. “Terminal sliding mode control design for air-breathing hypersonic vehicles.” *International Symposium on Systems & Control in Aeronautics & Astronautics IEEE*, 2010.

[7] Wang, P. , and Q. J. Liu . “Terminal sliding mode attitude controller design for a near-space hypersonic vehicle.” *IEEE Chinese Guidance, Navigation & Control Conference IEEE*, 2017.

[8] Zhai, Rongyu , R. Qi , and B. Jiang . “Fault-tolerant control for reentry hypersonic vehicle with blended aerodynamic surfaces and RCS.” *Control Conference IEEE*, 2016.

[9] Cheng, Xianlei , P. Wang , and G. Tang . “Reentry attitude tracking control for hypersonic vehicles with RCS,” *Chinese Control Conference* 2017.

[10] Wu sentang, “Flight Control System,” *Beijing university of aeronautics and astronautics press*, 2013.

[11] Zhi, Wang , S. Linan , and L. Huifeng, “Modeling of Non-redundant RCS System and Hybrid Control of High L/D Gliding Vehicle.” *Intelligent Control & Automation IEEE*, 2015.

[12] Shaughnessy, J D ,et al, “Hypersonic Vehicle Simulation Model: Winged-Cone Configuration,” 1990.

[13] Sun changyin, mu chaoxu, and zhang ruimin, “Terminal sliding mode control technology of hypersonic,” *Aircraft. Science press*, 2014.

[14] Zhang, Shengyan, et al. “Research on the Electromagnetic Valve of Reaction Control System with PWM Control Technology.” *Computer Measurement & Control* (2015).

[15] Hong, Yingdong, et al. "Reaction control system of hypersonic vehicle and its moment parameter identification." *Control Conference* 2014.

[16] Bandyopadhyay, B , and S. Janardhanan , “Sliding Mode Control in Electro-Mechanical Systems,” Second Edition, *Sliding mode control in electro-mechanical systems* .

[17] Liu jinkun, “Sliding mode variable structure control MATLAB simulation,” *Tsinghua University Press*, 2012.